Supplementary Information

Hollow Polyaniline Microsphere/Fe_3O_4 Nanocomposite as an Effective Adsorbent for Removal of Arsenic from Water

Soumi Dutta[1], *Kunal Manna*[2], *Suneel Kumar Srivastava*[2,3*], *Ashok Kumar Gupta*[1+], *Manoj Kumar Yadav*[4]

[1]School of Water Resources, Indian Institute of Technology Kharagpur, Kharagpur–721302, India

[2]Department of Chemistry, Indian Institute of Technology Kharagpur, Kharagpur–721302, India

[3]School of Energy Science and Engineering, Indian Institute of Technology Kharagpur, Kharagpur–721302, India

[4]School of Environmental Science and Engineering, Indian Institute of Technology Kharagpur, Kharagpur–721302, India

For Correspondence:

[*]S.K. Srivastava (sunil111954@yahoo.co.uk), [+]A.K. Gupta (agupta@civil.iitkgp.ac.in)

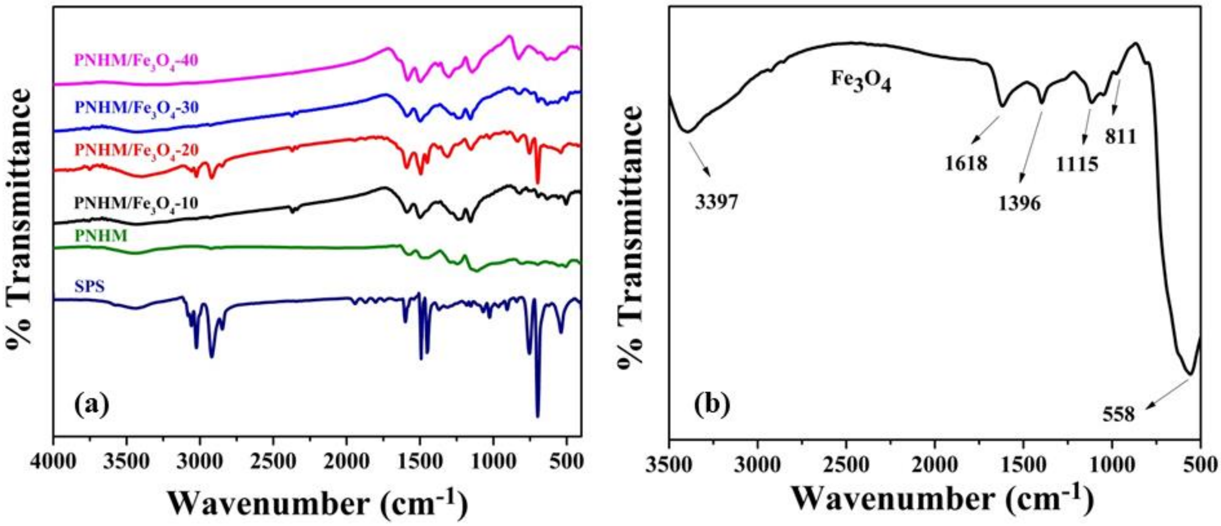

Figure S1. FTIR spectra of (a) SPS, PNHM and PNHM/Fe_3O_4 composites; (b) Fe_3O_4 nanoparticles.

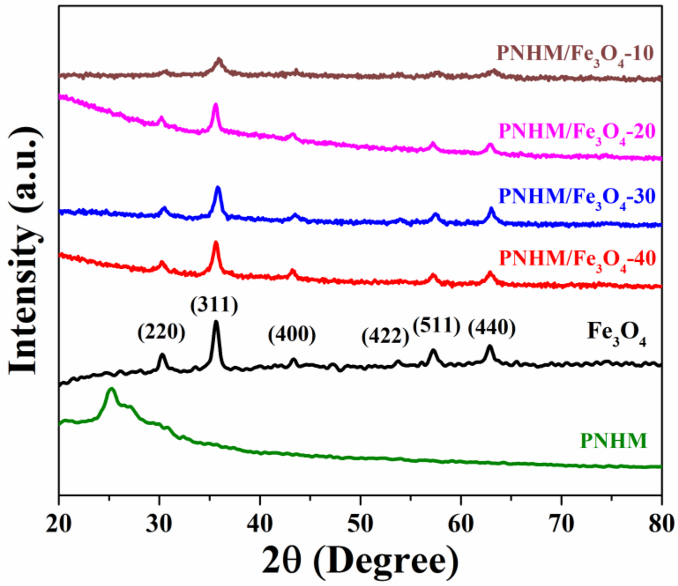

Figure S2. X-ray diffraction pattern of PNHM, Fe_3O_4 and PNHM/Fe_3O_4 composites.

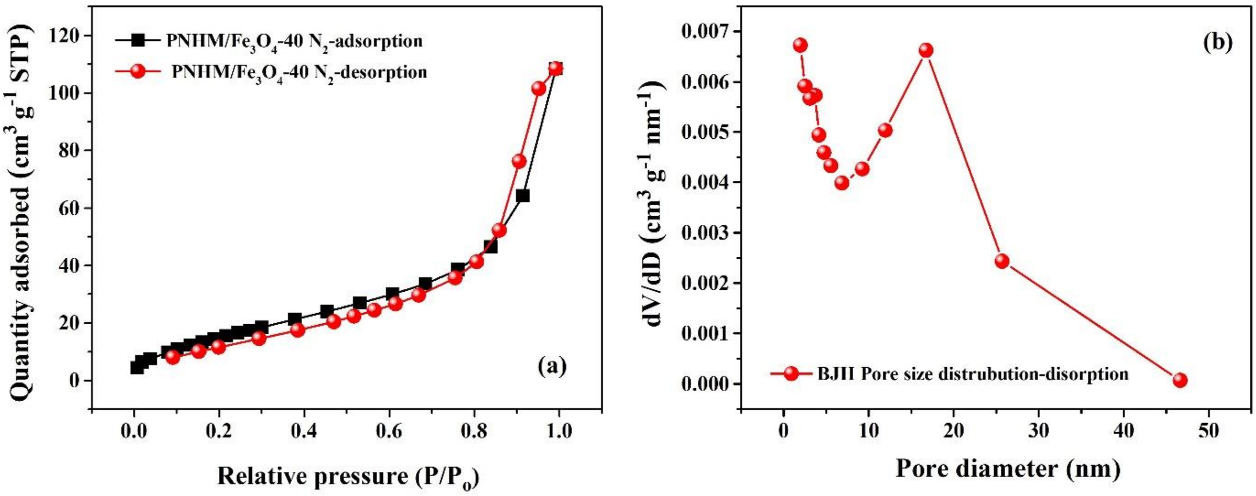

Figure S3. (a) N_2 adsorption–desorption isotherm measured for PNHM/Fe_3O_4–40; (b) BJH pore size distribution plot of PNHM/ Fe_3O_4-40.

Table S1. M_s, M_r, H_c values of Fe_3O_4 and PNHM/Fe_3O_4-40

Materials	Saturation magnetization, M_s (emu g^{-1})	Remanence, M_r (emu g^{-1})	Coercivity, H_c (Oe)
Fe_3O_4	~66.733	~4.293	~31.336
PNHM/Fe_3O_4–40	~24.398	~0.558	~30.837

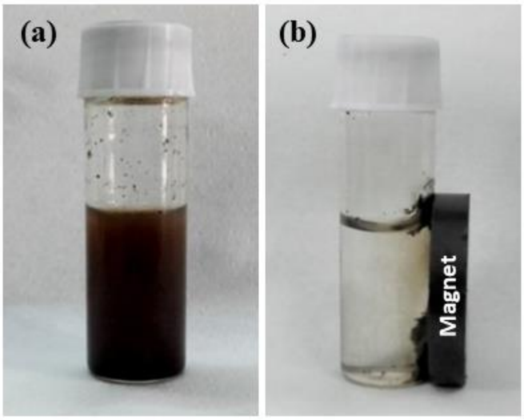

Figure S4. (a) Photos of PNHM/Fe_3O_4-40 dispersed in aqueous solution; (b) Separating by an external magnetic field.

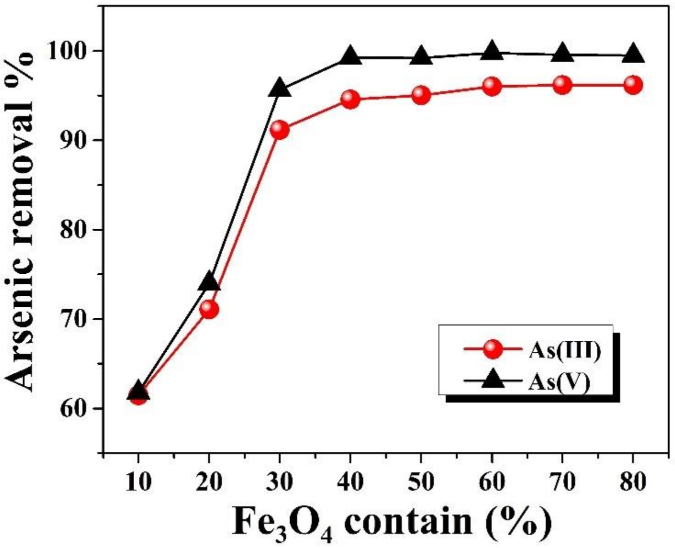

Figure S5. The effect of Fe_3O_4 content in PNHM/Fe_3O_4 nanocomposites on As(III) and As(V) uptake (Experimental conditions: C_0: 1000 µg L^{-1}; pH~7; adsorbent dose: 1g L^{-1}; contact time: 240 min; T: 300±3 K)

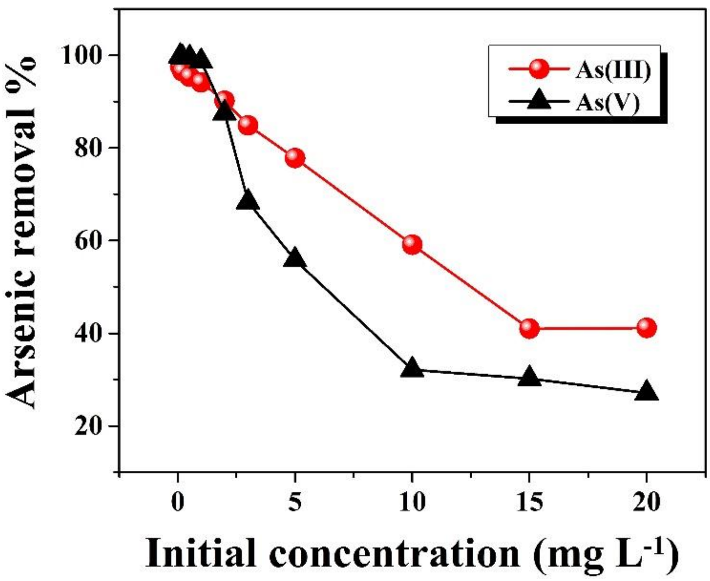

Figure S6. Effect of initial concentration of arsenic on removal efficiency (Experimental conditions: pH~7; adsorbent dose: 1g L^{-1}; Contact time: 240 min; T: 300±3 K).

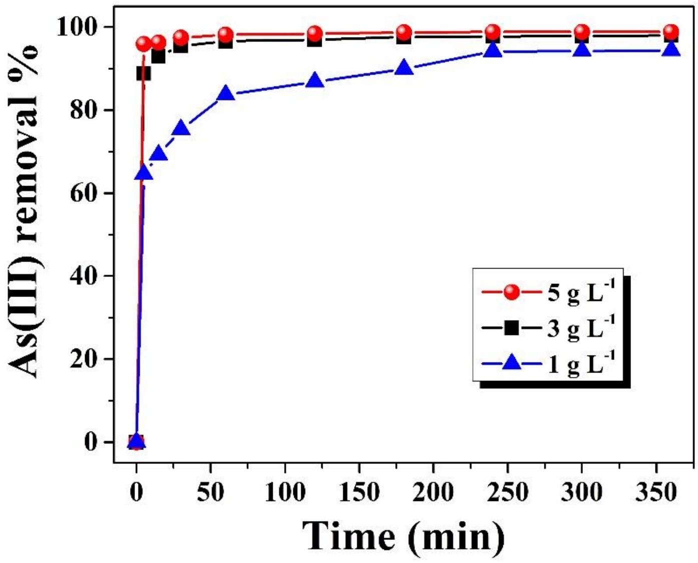

Figure S7. Effect of contact time on As(III) removal % at different adsorbent dose (1, 3, 5 g L^{-1}) with a fixed adsorbate concentration (1000 μg L^{-1}).

SI–1: Adsorption kinetics. The pseudo first-order kinetics model also referred as Lagergren first-order model, as following form[1,2]:

$$q_t = q_e(1 - e^{-k_1 t}) \quad (1)$$

where q_e and q_t indicates the amount arsenic uptake per unit weight (mg g^{-1}) of PNHM/Fe_3O_4-40 at equilibrium and any time t, respectively, and k_1 represents the rate constant (min^{-1}) of pseudo first-order model. Experimental data's are also fitted in the pseudo second-order kinetic model using the rate equation described by Ho and McKay[3] as follows:

$$q_t = \frac{(k_2\, q_e^2\, t)}{(1+k_2 q_e\, t)} \quad (2)$$

where k_2 is the pseudo second-order rate constant. The residual root means square error ($RMSE$) was used to measure the goodness-of-fit and was calculated by the following equation:

$$RMSE = \sqrt{\frac{\sum_{i=1}^{m}(Q_i - q_i)^2}{m}} \quad (3)$$

Where, Q_i and q_i indicates the observed data from the batch experiment and estimate data from kinetics and isotherm models, respectively. *m* is the number of observations taken in the experiment. It is observed that the smaller *RMSE* value indicates the better curve-fitting.

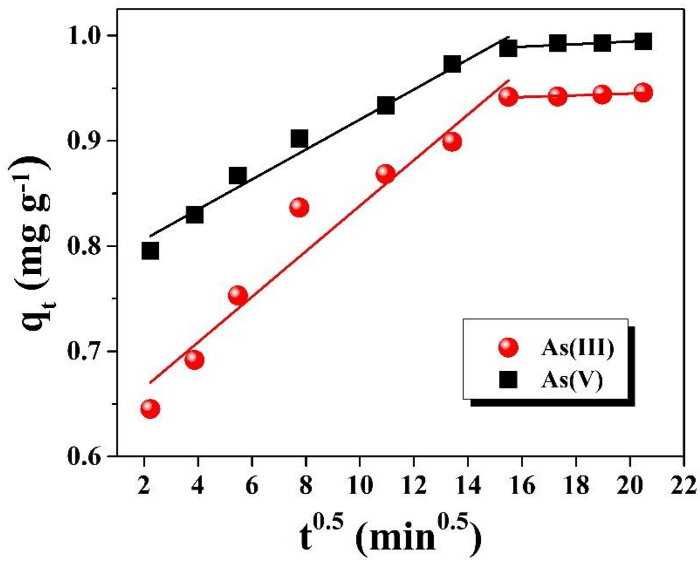

Figure S8. Kinetics data fitted to The Weber–Morris intra-particle diffusion plot for As(III) and As(V) adsorption on PNHM/Fe_3O_4-40 (Experimental conditions: adsorbent dose: 1g L^{-1}; C_0: 1000 µg L^{-1}; pH~7; T: 300 ± 3 K).

Table S2. Kinetic parameters for As(III) and As(V) adsorption on PNHM/Fe_3O_4-40

Kinetic models		Parameters	As(III)	As(V)
Pseudo first-order model		q_e (mg g^{-1})	0.877	0.943
		k_1 (min^{-1})	0.226	0.359
		R^2	0.919	0.964
		Adj. R^2	0.910	0.960
		RMSE	0.083	0.058
Pseudo second-order model		q_e (mg g^{-1})	0.916	0.966
		k_2 (g mg^{-1} min^{-1})	0.363	0.733
		R^2	0.969	0.983
		Adj. R^2	0.965	0.982
		RMSE	0.051	0.039
Intra-particle diffusion model	Steep slope	k_d (mg g^{-1} min$^{-0.5}$)	0.022	0.014
		C (mg g^{-1})	0.622	0.778
		R^2	0.950	0.979
		Adj. R^2	0.940	0.974
		RMSE	0.027	0.011
	Gradual slope	k_d (mg g^{-1} min$^{-0.5}$)	8.2×10^{-4}	0.001
		C (mg g^{-1})	0.929	0.969
		R^2	0.918	0.848
		Adj. R^2	0.877	0.772
		RMSE	6.5×10^{-4}	0.001

SI–2: Adsorption isotherm. Langmuir isotherm model is described below[4]:

$$q_e = \frac{Q_m\, b\, C_e}{1+b\, C_e} \tag{4}$$

where, b refers the Langmuir constant corresponding to the binding energy (L mg^{-1}) of the solute and Q_m is the maximum adsorption capacity (mg g^{-1}). In addition, Freundlich isotherm model has been used to describe adsorption of arsenic taking place on a heterogeneous surface[5] of PNHM/Fe_3O_4-40 is not restricted to monolayer formations and can be described as below:

$$q_e = K_f\, C_e^{\frac{1}{n}} \tag{5}$$

where, K_f and n are the Freundlich constant corresponding to the adsorption capacity [(mg g^{-1})(L mg^{-1})$^{1/n}$] and intensity of the adsorption, respectively.

Table S3. Isotherm parameters for As(III) and As(V) adsorption on PNHM/Fe_3O_4-40

Isotherm models	**Parameters**	**As(III)**	**As(V)**
Langmuir isotherm	Q_m (mg g^{-1})	28.265	83.078
	b (L mg^{-1})	0.015	0.002
	R^2	0.907	0.987
	Adj. R^2	0.901	0.986
	RMSE	3.047	2.212
Freundlich isotherm	K_f [(mg g^{-1})(L mg^{-1})$^{1/n}$]	3.145	1.057
	1/n	0.326	0.576
	R^2	0.984	0.999
	Adj. R^2	0.983	0.998
	RMSE	1.264	0.730

Table S4. Comparison of maximum adsorption capacity of the PNHM/Fe_3O_4-40 with other adsorbents for removal of arsenic (pH~7)

Type of adsorbent	Maximum adsorption capacity (mg g^{-1})		Ref.
	As(III)	**As(V)**	
Fe_3O_4 nanoparticles	46.06	16.56	6
α-Fe_2O_3	95.0	47.0	7
Fe_3O_4@Polyaniline	1.385	1.066	8
polyaniline/polystyrene nanocomposite	52	56	9
Nano Zero-Valent Iron on Activated Carbon	18.2	12.0	10
Porous Fe_3O_4	6.77	7.23	11
Commercial Fe_3O_4	0.76	1.35	11
Poly(lauryl methacrylate divinylbenzene)/poly(glycidyl methacrylate)/Fe_3O_4	53.97	-	12
Fe_2O_3@C	29.40	17.9	13
Fe_3O_4–Honeycomb briquette cinders	1.566	1.288	14
PNHM/Fe_3O_4-40	**28.27**	**83.08**	**Present study**

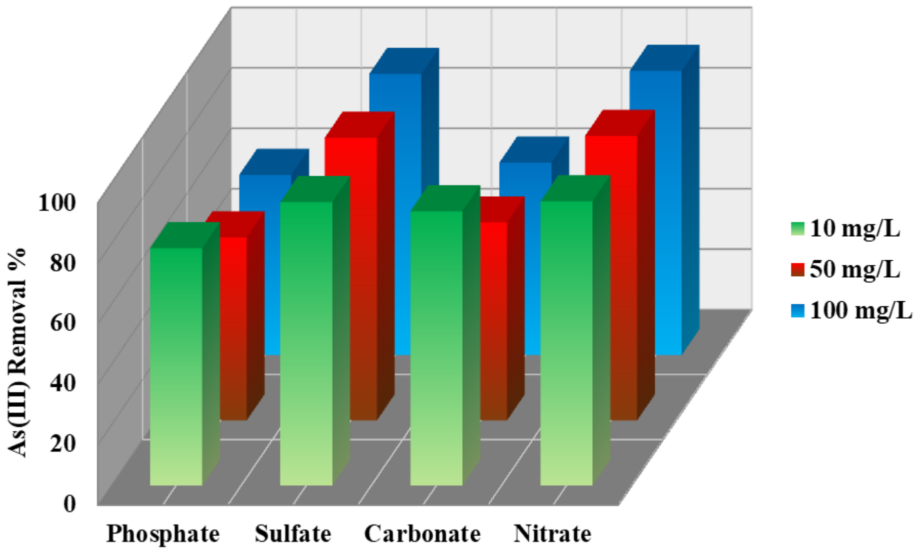

Figure S9. Effect of competing ions on removal of As(III) using PNHM/Fe_3O_4-40 (Experimental conditions: adsorbent dose: 1g L^{-1}; C_0: 1000 µg L^{-1}; T: 300±3 K; contact time: 240 min).

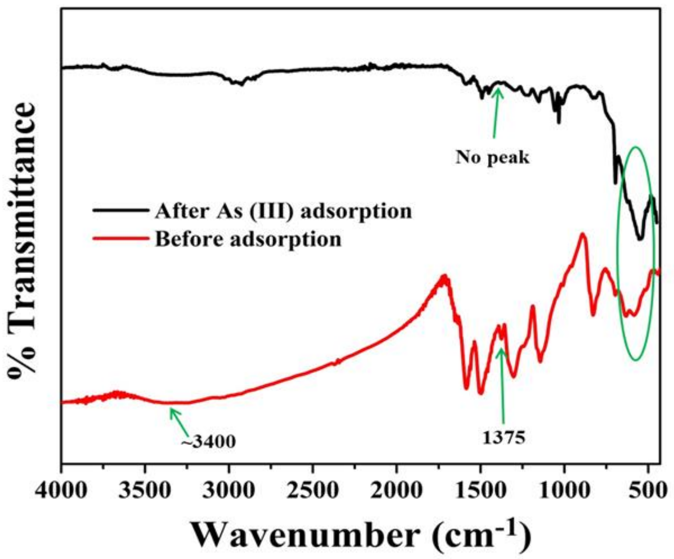

Figure S10. FTIR spectra of PNHM/Fe_3O_4-40 composite particles at before and after As(III) adsorption.

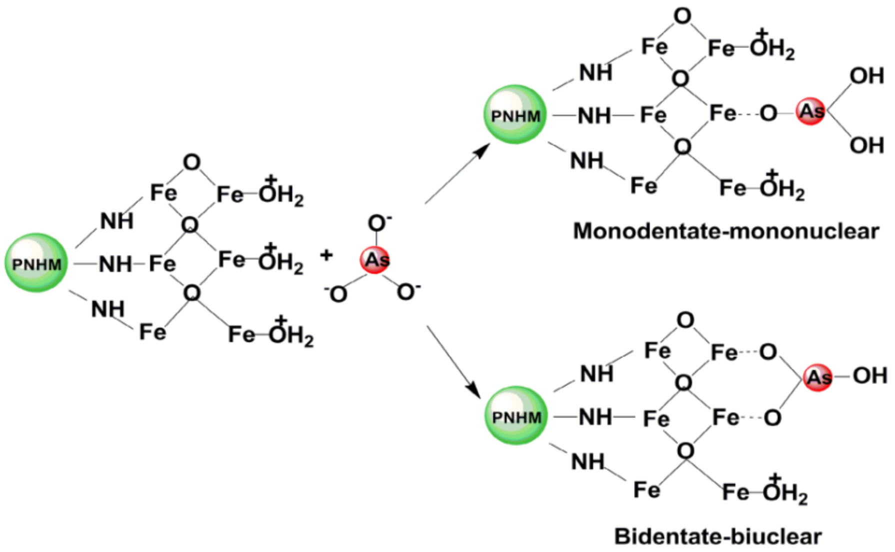

Figure S11. Probable mechanism of arsenic adsorption on PNHM/Fe_3O_4-40 at pH ~7.

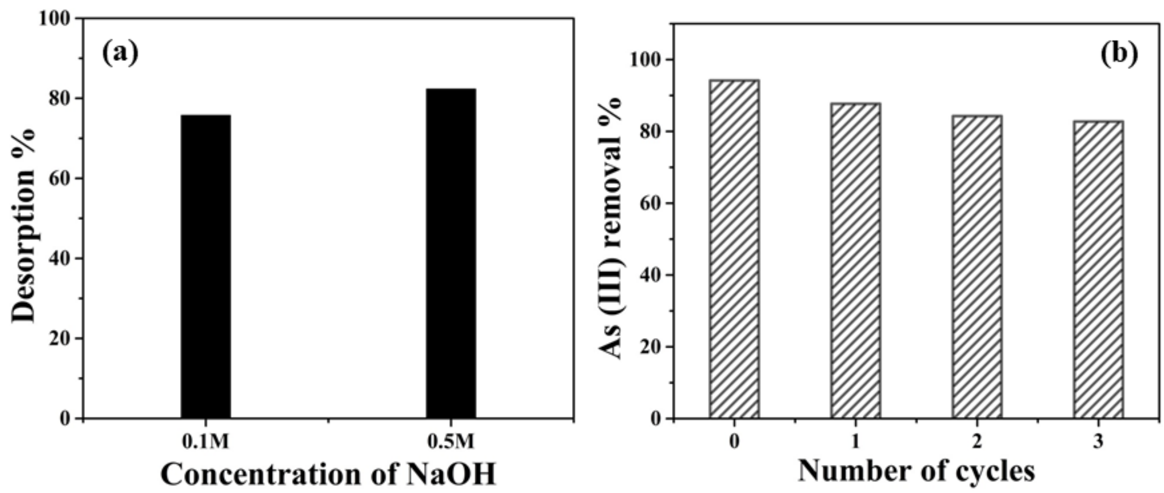

Figure S12. (a) Desorption of As(III) from loaded PNHM/Fe_3O_4–40 with different concentration of NaOH solutions; (b) As(III) removal % using regenerated PNHM/Fe_3O_4-40 upto three adsorption/desorption cycles (Experimental conditions: C_0: 1000 µg L^{-1}, dose 1g L^{-1}, T: 300±3 K , pH~7).

Table S5. Physicochemical parameters of naturally arsenic contaminated groundwater sample

Parameters	**Quantity**
Total arsenic (μg L^{-1})	152.54
Conductivity (μs cm^{-1})	2402
Total dissolved solid (mg L^{-1})	1404
Salinity (PSU)	1.09
pH	7.13
Turbidity (NTU)	59.27
Sodium (mg L^{-1})	239.348
Potassium (mg L^{-1})	273.596
Calcium (mg L^{-1})	65.920
Magnesium (mg L^{-1})	0.576
Chloride (mg L^{-1})	377.742
Phosphate (mg L^{-1})	1.153
Total alkalinity (mg L^{-1})	480
Total suspended solid (mg L^{-1})	41

REFERENCES

1. Ho, Y. S. & McKay, G. A Comparison of Chemisorption Kinetic Models Applied to Pollutant Removal on Various Sorbents. *Process Safety and Environmental Protection* **76**, 332–340 (1998).
2. Qiu, H. *et al.* Critical review in adsorption kinetic models. *Journal of Zhejiang University-Science A* **10**, 716–724 (2009).
3. Ho, Y. S. & McKay, G. Sorption of dye from aqueous solution by peat. *Chemical Engineering Journal* **70**, 115–124 (1998).
4. Bhaumik, M., Noubactep, C., Gupta, V. K., McCrindle, R. I. & Maity, A. Polyaniline/Fe^0 composite nanofibers: An excellent adsorbent for the removal of arsenic from aqueous solutions. *Chemical Engineering Journal* **271**, 135–146 (2015).
5. Srivastava, S. K., Senapati, S., Singh, S. B. & Raul, P. K. Magnetic Ni/PPy nanocomposite as effective reusable adsorbent for removal of arsenite and fluoride from contaminated water. *RSC Advances* **6**, 113424–113431 (2016).
6. Feng, L., Cao, M., Ma, X., Zhu, Y. & Hu, C. Superparamagnetic high-surface-area Fe_3O_4 nanoparticles as adsorbents for arsenic removal. *Journal of Hazardous Materials* **217–218**, 439–446 (2012).
7. Tang, W., Li, Q., Gao, S. & Shang, J. K. Arsenic(III,V) removal from aqueous solution by ultrafine α-Fe_2O_3 nanoparticles synthesized from solvent thermal method. *Journal of Hazardous Materials* **192**, 131–138 (2011).
8. Zhou, Q., Wang, J., Liao, X., Xiao, J. & Fan, H. Removal of As(III) and As(V) from water using magnetic core-shell nanomaterial Fe_3O_4@polyaniline. *International Journal of Green Technology* **1**, 54-64 (2015).
9. Davodi, B. & Jahangiri, M. Determination of optimum conditions for removal of As(III) and As(V) by polyaniline/polystyrene nanocomposite. *Synthetic Metals* **194**, 97–101 (2014).
10. Zhu, H., Jia, Y., Wu, X. & Wang, H. Removal of arsenic from water by supported nano zero-valent iron on activated carbon. *Journal of Hazardous Materials* **172**, 1591–1596 (2009).
11. Wang, T. *et al.* Controllable Synthesis of Hierarchical Porous Fe_3O_4 Particles Mediated by Poly(diallyldimethylammonium chloride) and Their Application in Arsenic Removal. *ACS Applied Materials & Interfaces* **5**, 12449–12459 (2013).
12. Shabnam, R. *et al.* Novel Magnetically Doped Epoxide Functional Cross-linked Hydrophobic Poly(lauryl methacrylate) Composite Polymer Particles for Removal of As(III) from Aqueous Solution. *Industrial & Engineering Chemistry Research* **56**, 7747–7756 (2017).
13. Wu, Z., Li, W., Webley, P. A. & Zhao, D. General and controllable synthesis of novel mesoporous magnetic iron oxide@carbon encapsulates for efficient arsenic removal. *Advanced Materials* **24**, 485–491 (2012).
14. Baig, S. A. *et al.* Arsenic removal from aqueous solutions using Fe_3O_4-HBC composite: effect of calcination on adsorbents performance. *PloS one* **9**, e100704 (2014).